

Integrated RTD – CFD Hydrodynamic Analysis for Performance Assessment of Activated Sludge Reactors

Sauro Manenti¹  · Sara Todeschini¹ ·
Maria Cristina Collivignarelli¹ · Alessandro Abbà¹

Received: 6 November 2017 / Accepted: 25 January 2018 / Published online: 8 February 2018
© Springer International Publishing AG, part of Springer Nature 2018

Abstract This work shows an integrated analysis method for hydrodynamic investigation of biological reactors for wastewater treatment in order to detect the amount and position of possible defects, such as bypass and dead volume, influencing process efficiency. To reach such a goal, the proposed methodology integrates Residence Time Distribution (RTD) analysis, providing global hydrodynamic information, with Computational Fluid Dynamics (CFD) analysis, showing local flow conditions. RTD analysis was performed through a time-discretized analytical model of in-series mixed-flow reactors with dead volumes and bypass. CFD analysis was carried out with a 3D finite volume model allowing the numerical solution of turbulent incompressible isothermal flow. The method was tested on a scale activated sludge pilot plant with pre-denitrification scheme made of two in-series tanks. Hydrodynamic tests were performed carrying out the stimulus-response experiment using clear water inside the reactor and lithium chloride as a tracer. Two operating conditions of practical interest were investigated: (i) no mixing and (ii) upstream mixing. The RTD analysis of the outflow curve of lithium concentration from the experiment allowed detecting: a) no bypass for both operating conditions, and b) 5% dead volume for condition (i). These results were confirmed by the CFD analysis that allowed

✉ Sauro Manenti
sauro.manenti@unipv.it

Sara Todeschini
sara.todeschini@unipv.it

Maria Cristina Collivignarelli
mcristina.collivignarelli@unipv.it

Alessandro Abbà
abba78@unipv.it

¹ Department of Civil Engineering and Architecture, University of Pavia, via Ferrata 1, 27100 Pavia, Italy

localizing the position of the dead volume. The integrated analysis proved to be effective for detection of both types and position of hydrodynamic defects. Therefore the proposed method can be adopted for performance assessment of activated sludge reactors and subsequent improvement of their efficiency.

Keywords Biological reactor · CFD analysis · RTD analysis · Bypass · Dead volume · Experimental validation

List of Main Symbols

E	Residence time distribution function [s^{-1}]
C	Tracer's concentration [$mg L^{-1}$]
i	Index of the mixed-flow reactor [-]
i_b	Bypass index [-]
i_d	Dead volume index [-]
M	Tracer's mass for pulse injection [kg]
N	Number of in-series mixed-flow reactors [-]
p	Pressure [Pa]
Q	Flow rate to the reactor [$m^3 s^{-1}$]
Q_b	Bypass flow rate [$m^3 s^{-1}$]
t	Physical time [s]
\bar{t}	Average hydraulic retention time [s]
T_{res}	Mean residence time [s]
V	Volume of the reactor [m^3]
V_d	Dead (or interchange) volume [m^3]
v_i	Cartesian components of average velocity [$m s^{-1}$]
x_i	Cartesian coordinates [m]
ν	Kinematic viscosity [$m^2 s^{-1}$]
ν_T	Eddy viscosity [$m^2 s^{-1}$]
Θ	Passive scalar concentration [$mg L^{-1}$]
ρ	Density [$kg m^{-3}$]
\mathbf{g}	Gravitational acceleration vector [$m s^{-2}$]
\mathbf{v}	Ensemble average velocity vector [$m s^{-1}$]
\mathbf{x}	Position vector [m]

List of Acronyms

CAS	Conventional activated sludge
CFD	Computational fluid dynamics
DEN	Upstream tank for nitrate removal
OX-NIT	Downstream tank for oxidation/nitrification
RANS	Reynolds averaged Navier-Stokes
RTD	Residence time distribution
SED	Settling tank
TAMR	Thermophilic aerobic membrane reactor
TKE	Turbulent kinetic energy
TSS	Total suspended solids
WWTP	Wastewater treatment plant

1 Introduction

In the field of environmental engineering, the performance assessment of biochemical treatment plants is of great concern. This topic is relevant to the management of both drinking water treatment plants (Sorlini et al. 2015a, b, c) and wastewater treatment plants (WWTPs) involving the conventional activated sludge (CAS) processes (Bertanza and Collivignarelli 2006) and other treatments such as disinfection (Collivignarelli et al. 2017a) and sludge dewatering (Bertanza et al. 2014). Their operation procedures have been significantly improved in the last century on the basis of both scientific and technical experiences in order to meet the specific requirements imposed by discharge limits (Hreiz et al. 2015; Todeschini et al. 2012; Todeschini et al. 2011; Collivignarelli et al. 2000) especially in case of wastewater reuse (Papa et al. 2016).

Anyway, the cost-effective management of these plants to match high treatment efficiency with suitable quality standard of the effluent is still an open challenge (Karpinska and Bridgeman 2016), especially considering the continuous increase of urbanization (Todeschini 2016) and recent climate trends affecting rainfall (Todeschini 2012).

Several studies prove that the treatment efficiency is equally determined by biological kinetics and the hydrodynamic behavior (Raboni et al. 2015; Meister et al. 2017). In few words, the same treatment efficiency can be obtained with reactors of different volume depending on the hydrodynamics and possible related deficiencies.

Among the techniques for testing the operating performance, those related to the hydrodynamic behavior of treatment plants are of great importance (Collivignarelli et al. 1995). The tests for hydrodynamic behavior assessment can be performed for each step of the treatment sequence through well-established theoretical and technical knowledge in the field of chemical engineering (Levenspiel 1999) that has been extended to environmental engineering.

The residence time distribution (RTD) method (Nauman 2007) has been successfully applied to pilot plants for biological nutrient removal (Newell et al. 1998) and its adoption for the analysis of the hydrodynamic behavior of CAS reactors inside the treatment plants can strongly influence both performance assessment and management criteria, revealing relevant hydrodynamic deficiencies that may affect a number of facilities, such as some diffuse types of non-ideal flows that are due to dead volumes and bypass.

Dead volume denotes the portion of the compartment where the reaction can not take place; possible reasons are due to sediment deposition or, more frequently, hydrodynamic malfunctioning that leads to stagnant regions and recycling of fluid. As a consequence, the mean residence time of the fluid particles inside the dead volume is, at least, one order of magnitude higher than the average hydraulic retention time that is the ratio of the reactor's volume to the inflowing rate.

As concerns the aerobic biological reactors for organic dissolved matter removal, the lacking at least of one of the three reactants (i.e. dissolved organic substrate, biomass, oxygen) in a part of the compartment involves an inhibition of the reaction in that zone which behaves like a dead volume.

Some authors (Collivignarelli and Bina 1993; Collivignarelli et al. 1995; Gallati et al. 2007) have shown a large amount of dead volume both in the biological reactors (of the order of 20–30%) and in the sludge digesters (up to 50%). These functional deficiencies are frequently the main reasons for the reduced efficiency of a treatment plant. The greater the dead volume the lower the actual average retention time; in some cases, the actual retention time falls below the minimum threshold required for assuring acceptable treatment level.

Bypass denotes a hydraulic short-circuiting that occurs when significant part of the inflowing rate exits the reactor within a time considerably lower than the average retention time. In this case, the overall efficiency of the WWTP is significantly reduced, as the bypassed flow rate is not subjected to biological reactions.

These hydraulic malfunctions are of great concern since they strongly affect: a) reliable operation of WWTPs and their efficiency, b) quality of the effluent, c) investment and operating costs to meet effluent quality standards.

The “diagnostic phase” of the RTD analysis allows quantifying both amount and type of the functioning deficiency affecting the process. A subsequent “corrective phase” is necessary to investigate how this deficiency can be reduced or eliminated in order to improve the treatment efficiency by means of some practical interventions that are relatively simple and cheap to realize (e.g., partition walls, deflectors, impellers etc.). Since these interventions are generally empirical and based on personal experience, there is the need for a standardized method integrating the “global” information, provided by RTD method, with “local” flow field conditions (Collivignarelli et al. 1995).

In order to reach such a goal, it is useful to adopt complementary investigation techniques, that could be both experimental and numerical, allowing a “local” description of the flow field (Karpinska and Bridgeman 2016) and providing the spatial distribution of the local mean residence time of the fluid (Baléo and Le Cloirec 2000; Manenti et al. 2017).

In the last two decades Computational Fluid Dynamics (CFD)-aided modeling has gained popularity over traditional wastewater treatment approaches, thus becoming quite useful in enhancing the performance of CAS reactors (Karama et al. 1999; Kjellstrand et al. 2005) helping the analysis of complex multiphase multi-component flows with heat transfer (Kochevsky 2004; Le Moullec et al. 2008). Several factors contribute to the increasing popularity of numerical modeling in engineering practice, as it is a cost- and time-efficient solution that allows evaluating process performance, isolating and quantifying possible bottlenecks in the system, predicting the potential consequences of the proposed corrective interventions before their implementation (Le Moullec et al. 2010a, b; Pereira et al. 2012; Morchain et al. 2014).

The CFD-aided modeling is a helpful tool that can sustain the design of a new facility and support other investigation instruments for the optimization or retrofitting of existing facilities devoted to wastewater treatment (Do-Quang et al. 1998; Essemiani et al. 2004; Guimet et al. 2004; De Gussem et al. 2014; Laurent et al. 2014).

This work illustrates an integrated approach that is based on a combined use of RTD and CFD analyses for quantifying and localizing possible hydrodynamic malfunctioning in a biological reactor. The proposed method is applied to a CAS reactor (with pre-denitrification scheme) in a pilot plant that is a scale model reproducing a widespread scheme of WWTP for both organic matter and nitrogen removal. Therefore, this integrated methodology shows a general usefulness in that it may help improving the treatment efficiency of similar facilities.

Owing to the problem complexity, at this stage of investigation, a simplified functioning condition of the reactor has been considered as it has been supplied with clear water and no air for biochemical reaction during the functioning. Besides keeping control of the relevant hydrodynamic aspects, in this way the complexity of numerical model has been maintained to a suitable level because simulating the actual rheological properties of the sludge would require an advanced modeling approach (Manenti et al. 2016; Todeschini et al. 2010). These aspects are of concern in the actual behavior of the reactor: for this reason an attempt to

simulate isothermal steady turbulent flow of a non-Newtonian fluid has been made. The development of a non-Newtonian hydrodynamic model requiring experimental validation will be the subject of an ongoing research and will be considered in a future study to account for non-Newtonian behavior of the sludge.

In the following, the relevant features of the investigated pilot plant are illustrated and the experimental RTD analysis of the CAS reactor is described. The basic theoretical aspects of RTD method are recalled and then the discrete tank-in-series model used to interpret the results from the RTD analysis is illustrated. The relevant features of the three-dimensional numerical model for simulating the hydrodynamics of the CAS reactor are shown. The results of the analyses are discussed integrating RTD and CFD outputs to point out hydrodynamic malfunctioning. The main conclusions are finally discussed.

2 Materials and Methods

2.1 Description of the Pilot Plant

The investigated experimental facility is a scale activated sludge pilot plant with pre-denitrification scheme made of two in-series tanks with a total volume of about $V = 0.45 \text{ m}^3$.

The supply tank of the pilot plant has a capacity of 1.0 m^3 and assures to the in-series tanks a constant inflow rate of $Q_{in} = 20 \text{ L h}^{-1}$ supplied through a peristaltic pump.

The upstream tank (DEN) is devoted to nitrate removal (denitrification), while the downstream tank (OX-NIT) operates oxidation/nitrification.

The output of the oxidation/nitrification tank is partly recirculated ($Q_{m-1} = 60 \text{ L h}^{-1}$) with a peristaltic pump at the inflow of the denitrification tank, while the remaining part is transferred to a settling tank (SED) with volume $V_{s-1} = 0.1 \text{ m}^3$.

In order to reproduce the CAS scheme (with the sludge recirculation from settler to oxidation tank), the clear water from the settling tank is recirculated (with a peristaltic pump) at the inflow of the denitrification tank with a constant flow rate $Q_s = 60 \text{ L h}^{-1}$. The clarified water is conveyed to a storage tank with volume $V_s = 0.6 \text{ m}^3$ at constant flow rate $Q_{out} = 20 \text{ L h}^{-1}$.

The layout of the plant is reported in Fig. 1.

The total inflowing rate to the in-series tanks is therefore $Q = Q_{in} + Q_{m-1} + Q_s = 140 \text{ L/h}$, the average hydraulic retention time of the denitrification-oxidation/nitrification tanks is about $\bar{t} = V/Q = 3 \text{ h}$.

Both the denitrification and the oxidation/nitrification tanks are equipped with an impeller and diffusers devoted to air supply (1 plate in the denitrification tank and 4 in the oxidation/nitrification). It must be pointed out that the diffuser plate in the denitrification tank is ordinarily turned off when the plant is functioning according to pre-denitrification scheme; but this plate could be occasionally turned on to increase the oxidation-nitrification volume in order to enhance the plant versatility.

Two hydrodynamic tests were performed with the use of clear water: in the first test no mixing conditions were assumed (all impellers and diffusers turned off); in the second test only the upstream impeller was turned on.

Each test was carried out using lithium chloride as tracer (5 g dosage) with a slug-dose (pulse input) method: the instantaneous dose of lithium chloride was added at the entrance of the denitrification tank and the tracer was sampled at the effluent of oxidation/nitrification tank

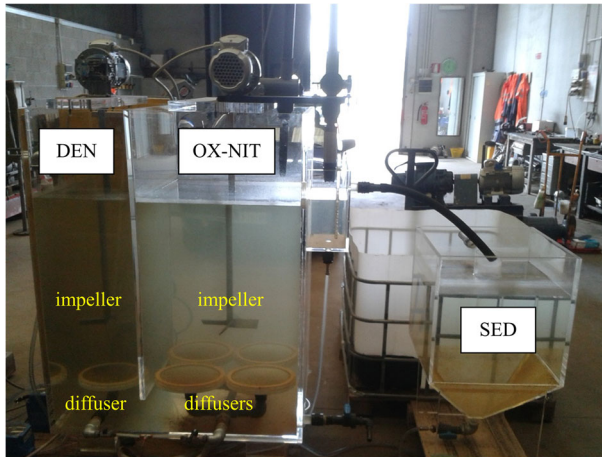


Fig. 1 Layout of the pilot plant

at certain time intervals. The testing period, for each experiment, is equal to 6 h (about 2 times the average hydraulic retention time of the system).

As previously said, a recirculation of the flow has been considered in order to reproduce the operating conditions of a CAS process with a pre-denitrification scheme. For this reason, tracer sampling was also carried out for the recirculation lines (the first from settler to denitrification tank and the second from oxidation/nitrification to denitrification tank) in order to take into account the amount of lithium chloride that comes back to the in-series tanks. So, the operating conditions simulated a CAS process with a pre-denitrification scheme.

All the samples collected during the tests were analysed for measuring lithium concentrations according to standard methods (APHA, AWWA, WEF 2012).

2.2 RTD Model

According to the general theory (Levenspiel 1999), each fluid particle takes different lengths of time to pass the tank (or reactor) depending upon the actual hydraulic path followed by the particle. This time length is usually referred to as exit age or residence time.

The Residence Time Distribution curve, frequently denoted by $E(t)$, indicates the exit age statistical distribution of all fluid particles passing the reactor. The RTD curve has the units of the inverse of time and is characterized by the following properties:

$$\int_0^{\infty} E(t) dt = 1$$

$$\bar{t} = \int_0^{\infty} t \cdot E(t) dt = \frac{V}{Q} \quad (1)$$

From Eqs. (1) it can be seen that: a) the area under the curve is unitary and b) the first order moment of the function $E(t)$ corresponds to the mean hydraulic residence time \bar{t} of a reactor with volume V and inflow rate Q .

The RTD curve is based upon the assumption that fluid particles passing the reactor can cross its boundary no more than one time. Therefore, the fraction of fluid particles leaving the reactor with an exit age between t and $t + dt$ is given by $E(t) dt$.

The experimental evaluation of the function $E(t)$ is based upon the so called stimulus-response experiment, that is the evaluation of the system (reactor) response to a hydraulic input that is obtained by injecting a tracer at the tank inflow. The output response is evaluated by analyzing the time evolution of tracer’s concentration in the outflow of the tank. The tracer may be reactive or non-reactive.

The tracer can be introduced at the inflow of the reactor in a simple manner, as in the cases of pulse input or step input that are easier to interpret. In some cases, other methods for the tracer’s injection could be conveniently adopted, such as periodic input and random input.

Since in this work the hydrodynamic analysis of the pilot plant has been carried out by using an almost instantaneous injection of non-reactive tracer, the pulse input is briefly recalled.

Ideally, the pulse input is represented by the Dirac delta function and all the tracer elements enter the reactor at the same time. Therefore, in the particular case of pulse input the $E(t)$ curve is the $C(t)$ curve (denoting the tracer concentration leaving the reactor at time t) scaled by a factor M/Q :

$$E(t) = \frac{C(t)}{M/Q} \tag{2}$$

For ideal plug flow and mixed flow subjected to pulse input, the analytical expression of $C(t)$ can be easily obtained.

To analyze the hydrodynamic behavior of the pilot plant, more complex analytical models of the RTD curve should be adopted. These models can be obtained by considering in-series and/or parallel arrangement of the elementary models, such as those previously described, possibly including bypasses, dead volumes and recirculation.

Figure 2 shows a general configuration of the analytical model consisting of N in-series mixed-flow reactors each having an interchange volume equal to $V_{d\ i}$ in order to account for dead volume. The possibility of a bypass flow rate Q_b is also represented in the sketch of Fig. 2.

In order to account for possible tracer recirculation occurring in the pilot plant, the analytical model is applied in a discretized form (i.e., time discretization). The discretized form can be easily implemented in a computer program to simulate the stimulus-response experiment carried out on the pilot plant. The outflowing tracer concentration from the i -th reactor after a time step Δt can be obtained by:

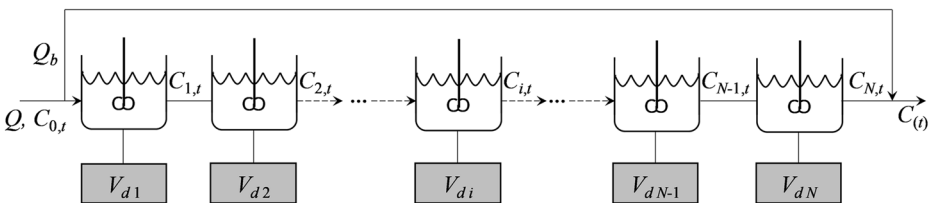


Fig. 2 Sketch of the discrete model simulating in-series mixed-flow reactors with dead volumes and bypass ($V_{d\ i}$: dead volume; Q_b : bypass flow rate)

$$\begin{aligned}
 C_{i,t+\Delta t} &= C_{i,t} + \left(\frac{C_{i-1,t} + C_{i-1,t+\Delta t} - C_{i,t}}{2} \right) \left[1 - \exp\left(-\frac{\Delta t(1-i_b)}{\bar{t}_i(1-i_d)} \right) \right] \\
 C_{i,0} &= C_{0,0} + \frac{i}{N} (C_{N,0} - C_{0,0}) \\
 C_{N,0} &= \frac{C_{0,0} - i_b C_{0,0}}{1 - i_b} \\
 C_{i+\Delta t} &= i_b C_{0,t+\Delta t} + (1 - i_b) C_{N,t+\Delta t}
 \end{aligned}
 \tag{3}$$

In Eqs. (3), \bar{t}_i denotes the mean hydraulic residence time of each reactor, $i_b = Q/Q_b$ is the bypass index, and $i_d = V/V_d$ is the dead volume index.

With the time-discretized model it is possible to account for recirculation with throughflow from the oxidation-nitrification compartment to the denitrification compartment. This goal is accomplished by considering that, after the pulse injection, the inflow concentration of lithium tracer $C_{0,t}$ for the first reactor in the series varies over time according to the concentration of the samples collected from the recirculating flow.

The above described discrete model has been adopted for RTD analysis of the pilot plant. The number of reactors, as well as their dead volumes, and the bypass flow rate represent tuning parameters to fit the time evolution of lithium concentration $C_{(t)}$ at the outflow of the reactor series with the experimental points sampled at different instants at the outflow of the oxidation/nitrification tank in the pilot plant.

The tank geometry of the pilot plant as well as the positioning of both inflow and outflow sections have been carefully designed to avoid formation of bypasses. This is confirmed by the results of the RTD analysis: as it will be shown in the following, the behavior of the discrete model fits reasonably well the experimental time evolution of lithium concentration sampled at the outflow of the oxidation/nitrification tank when zero bypass flow rate is assumed in the discrete model.

2.3 CFD Model

This section describes the relevant features of the numerical model for the hydrodynamic analysis of the pilot plant.

The commercial code STAR-CCM+ (v.7.04.006) is adopted for the numerical solution of turbulent incompressible isothermal flow with RANS model:

$$\begin{aligned}
 \nabla \cdot \mathbf{v} &= 0 \\
 \frac{\partial \mathbf{v}}{\partial t} + \mathbf{v} \cdot \nabla \mathbf{v} &= -\frac{1}{\rho} \nabla p + (\nu + \nu_T) \nabla^2 \mathbf{v} + \mathbf{g}
 \end{aligned}
 \tag{4}$$

In Eqs. (4), \mathbf{v} denotes the ensemble average velocity vector of the mean flow field, ρ and p are the fluid density and pressure respectively, ν is the kinematic viscosity of the fluid, and \mathbf{g} is the gravity acceleration. The eddy viscosity ν_T accounts for the turbulent effects.

In the finite volume method (Hirt and Nichols 1981), the computational domain is divided into a discrete number of control volumes representing the computational grid. The integral form of the conservation Eqs. (4) applied to each control volume is discretized, thus obtaining a set of linear algebraic equations in which the number of unknowns matches the number of cells in the computational grid. A second order upwind finite volume scheme is adopted for computing the convective flux.

The conservation equations for the pressure and for the velocity are solved in an uncoupled manner (segregated flow option) and then the linkage between the momentum and continuity equations is achieved through the predictor-corrector method SIMPLE (Patankar and Spalding 1972).

The closure of the conservation Eqs. (4) is obtained with the standard $k-\varepsilon$ model (Launder and Spalding 1974) previously adopted in analogous problems simulating the fluid flow in treatment plants (Morchain et al. 2000). Such a model is a standard version of the model involving two balance differential equations for specific turbulent kinetic energy k (TKE) and its specific dissipation rate ε :

$$\begin{aligned} \frac{\partial k}{\partial t} + v_j \frac{\partial k}{\partial x_j} &= \frac{\partial}{\partial x_j} \left[\left(\frac{v_T}{\sigma_k} + v \right) \frac{\partial k}{\partial x_j} \right] + v_T \left(\frac{\partial v_i}{\partial x_j} + \frac{\partial v_j}{\partial x_i} \right) \frac{\partial v_i}{\partial x_j} - \varepsilon \\ \frac{\partial \varepsilon}{\partial t} + v_j \frac{\partial \varepsilon}{\partial x_j} &= \frac{\partial}{\partial x_j} \left[\left(\frac{v_T}{\sigma_\varepsilon} + v \right) \frac{\partial \varepsilon}{\partial x_j} \right] + C_{1\varepsilon} \frac{\varepsilon}{k} v_T \left(\frac{\partial v_i}{\partial x_j} + \frac{\partial v_j}{\partial x_i} \right) - C_{2\varepsilon} \frac{\varepsilon^2}{k} \end{aligned} \tag{5}$$

The symbol v_i denotes the Cartesian components of the average velocity \mathbf{v} in the coordinate system x_i ($i = 1, 2, 3$); summation convention is assumed for repeated indices. The empirical coefficients in the transport Eqs. (5) are assumed as follows (Rodi 1980; Patel et al. 1985): $C_{1\varepsilon} = 1.44$, $C_{2\varepsilon} = 1.9$, $\sigma_\varepsilon = 1.3$, $\sigma_k = 1.0$. The local value for the turbulent coefficient ν_T in Eqs. (4) and (5) is given by:

$$\nu_T = C_\mu \frac{k^2}{\varepsilon} \tag{6}$$

The empirical coefficient in Eq. (6) is set equal to $C_\mu = 0.09$.

The numerical solution of the governing Eqs. (4) allows to calculate the hydrodynamic flow inside the reactor (Brouckaert and Buckley 1999).

The symmetry of the pilot plant with respect to the vertical longitudinal mid-plane has been used to simulate only half part of the facility, thus reducing the computational effort; for consistency, the flow rate entering the reactor is assumed to be half the inflowing rate of the pilot plant (see Table 1).

The model geometry is shown in Fig. 3 and schematizes the actual geometry of half the pilot plant (see Fig. 1).

The 3D computational domain has been discretized by means of polyhedral meshes, that provide a balanced solution for complex geometries, and the result is shown in the right-hand panel of Fig. 3. The surface remesher option is activated to create high quality volume mesh; a minimum face quality of 0.05 was found to assure acceptable computational cost and suitable result quality. A base size of 0.01 m has been selected as characteristic dimension of the model’s geometry.

Table 1 Values of the relevant model’s parameters

Parameter	Value
Fluid density	1000 kg m ⁻³
Dynamic viscosity	1.0E-3 Pa s
Reference pressure	101,325.0 Pa
Inflowing rate*	1.94E-5 m ³ s ⁻¹
n. control volumes*	315,725

*These values are referred to the half-reactor (see Fig. 3)

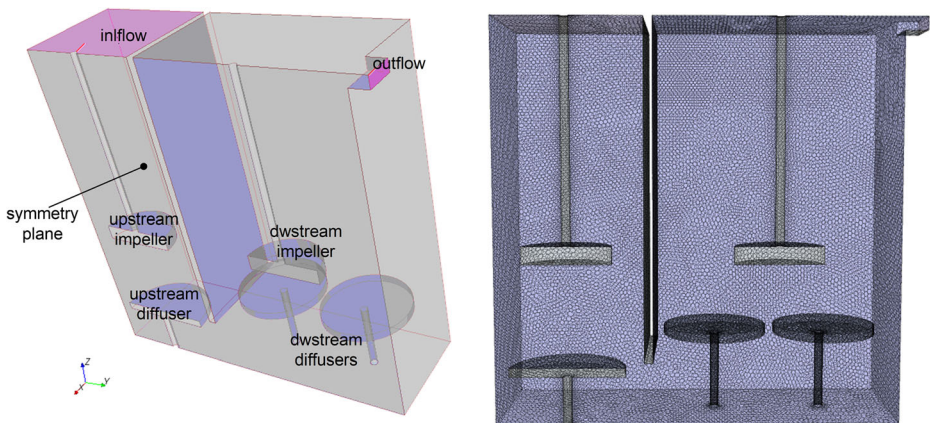


Fig. 3 Geometry and mesh discretization of the simulated half-reactor

Proper boundary conditions have been assigned to the surfaces surrounding the half-reactors (Fig. 3). The inflow upper left surface simulates a velocity inlet normal to the boundary with a constant rate of $1.84\text{E-}4 \text{ m s}^{-1}$: in this way, the same inflow rate of the scale pilot plant tested in this work can be obtained (note that the numerical model simulates half the volume of the reactor, and therefore, one half of the overall inflow rate is considered, see Table 1). The outflow surface on the right-hand side simulates a pressure outlet with constant relative pressure equal to 0.0 Pa. The frontal vertical side simulates an imaginary plane of symmetry, and therefore, the calculated solution is identical to the one that would be obtained when assuming the full geometry by mirroring the mesh about the symmetry plane outside the computational domain.

The effect of air bubbles (potentially released from the bottom membrane disc type diffusers) is neglected at this stage of investigation in which single-phase flow of clear water has been simulated with the aim of examining the reactor hydrodynamics without increasing the model complexity. Further studies will account for the presence of both activated sludge and gaseous dispersed phase by carrying out multiphase flow analysis of non-Newtonian fluids.

Each mixing device is simulated by an equivalent cylinder with the same overall dimensions of the rotating impeller in the pilot plant. The functioning condition with the upstream impeller turned on has been simulated by assuming an inlet boundary condition with normal velocity of 0.1 m s^{-1} at the upper and lower faces of the cylinder in order to mimic upward continuous fluid flow across the impeller. The adopted velocity value of 0.1 m s^{-1} is representative of the operating condition of the impeller.

Impermeable wall boundary condition has been imposed on the remaining surfaces of the reactor.

Table 1 summarizes the relevant model parameters adopted in the computation.

The local mean residence time of a fluid particle, that occupies a given point within the steady flow field, has the physical meaning of the average time to reach that point since this particle entered the reactor inlet (Sandberg 1981).

Once the stationary flow field has been calculated by solving the balance Eqs. (4) coupled with the turbulence transport Eqs. (5), the mean residence time is evaluated through the passive scalar method solving a transport equation without source term for the passive scalar component (Warhaft 2000):

$$\frac{\partial \Theta}{\partial t} + \mathbf{v} \cdot \nabla \Theta = \left(\frac{\mu}{\sigma} + \frac{\mu_T}{\sigma_T} \right) \nabla^2 \Theta \quad (7)$$

In Eq. (7), Θ denotes the passive scalar field, σ and σ_T are, respectively, the laminar and turbulent Schmidt numbers influencing the scalar's diffusivity. The diffusive effects on the residence time computation are evaluated assuming the turbulent Schmidt number equal to $\sigma_T = 0.7$ (Le Moulec et al. 2008).

In the present study that considers a steady-state flow, the local time derivatives at the left-hand member of Eqs. (4), (5) and (7) are neglected.

In all the computations the hydrodynamic steady field is computed first without the passive scalar model until the computation has converged (typically, this is obtained within about 150 iterations). Subsequently, passive scalar is activated initializing its value to zero over the entire computational domain and at the inflow boundary.

3 Results and Discussion

The numerical model previously described has been adopted for carrying out steady-state hydrodynamic analysis of the pilot plant.

At this early stage of investigation the hydrodynamic analysis of the pilot plant has been carried out considering clear water throughflow without air injection from the bottom diffusers. These assumptions represent a simplification with respect to the operating conditions of the plant involving a suspension of activated sludge with air bubbles. Simulating such a multi-phase problem involving non-Newtonian fluid would require a higher complexity of the numerical modeling as well as input data (such as sludge rheological parameters) that will be provided by a companion research still in progress (Abbà et al. 2017).

For these reasons, a single-phase steady hydrodynamic analysis of Newtonian fluid has been performed with the aim of checking the numerical model. This goal is accomplished by evaluating the mean residence time distribution inside the reactor's volume for quantitative comparison with the RTD analysis that has been performed on the pilot plant operating with clear water, without air supply and with the absence of biomass.

Two different operating conditions of the pilot plant have been modeled: (i) “no-mixing” analysis in which both upstream and downstream impellers are turned off, and (ii) “upstream mixing” analysis in which the upstream impeller is operating while downstream impeller is turned off. These two functioning conditions have been adopted during the experimental tests on the pilot plant in order to assess the influence of mixing process on the overall hydrodynamic behavior of the reactor.

Figure 4 shows the results obtained from the numerical model for the two types of analyses carried out. The continuous red curve refers to “no-mixing” condition, while dashed blue curve has been obtained considering the upstream impeller turned on. The ordinate of a generic point on these curves indicates the volume fraction of the reactors in the pilot plant with a calculated residence time greater or equal than the time corresponding to the abscissa of that point. The black dashed vertical line has been traced at $T_{res} = 30$ h, i.e., one order of magnitude of the average hydraulic retention time \bar{t} of the pilot plant, that represents a limit for evaluating the percentage of dead volume (Levenspiel 1999; Collivignarelli et al. 1995).

Concerning the analysis with upstream impeller turned on (blue-dashed line), it can be noticed that this curve is made up of two down-sloping tracts connected by a sub-horizontal

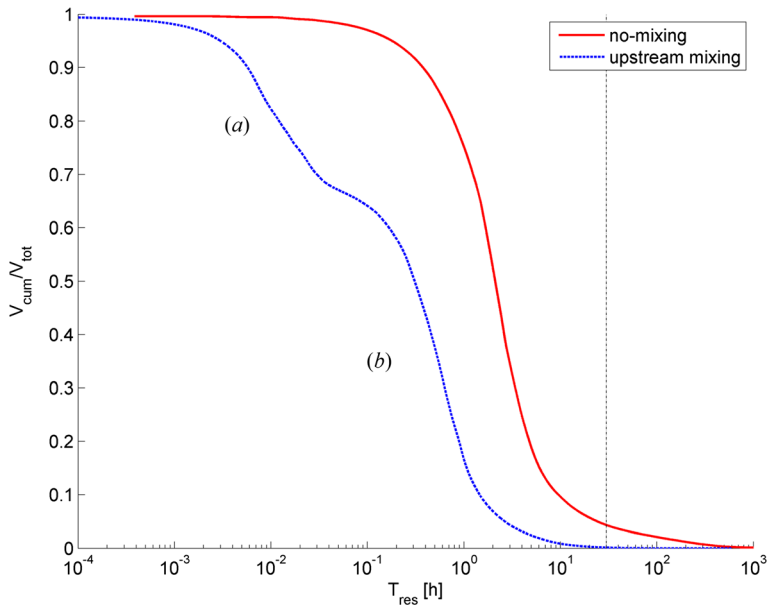


Fig. 4 Distribution curves of mean residence time as percentage of reactor volume for two operating conditions: “no-mixing” and “upstream mixing”

segment. The upper down-sloping tract, denoted with (a) in Fig. 4, is representative of a volume portion (about one third of the total volume) which is characterized by a mean residence time smaller than about 2 min and coincides with the denitrification tank where the mixing effect of the upstream impeller increases the fluid velocity magnitude and is responsible for the very small value of the mean residence time compared to the average hydraulic retention time. The lower down-sloping tract of the dashed blue curve, denoted with (b) in Fig. 4, is representative of the hydraulic behavior of the oxidation/nitrification tank (about two-third of the total volume) where the mean residence time increases to about 1 h with respect to the denitrification tank owing to the absence of direct mixing. However, the fluid particles coming from the denitrification tank are characterized by a higher velocity magnitude, and therefore, they contribute to increase of the linear momentum of the fluid within the oxidation/nitrification tank: for this reason, only a small portion of the volume in the oxidation/nitrification (about 4% with respect to the total volume) has a mean residence time greater than the average hydraulic retention time $\bar{t} = 3$ h. Accordingly, the ordinate of the point of the curve with abscissa $T_{res} = 30$ h shows that the estimated amount of dead volume (within the oxidation/nitrification tank) is about 0.2% of the total volume, which is quite negligible.

The distribution curve obtained with both impellers turned off (red continuous line) is shifted forward with respect to the previous case and shows a single down-sloping tract. This analytical behavior is due to the fact that, when mixing is absent, the average velocity magnitude of the fluid particles in both compartments is almost similar (see Fig. 6) and, on average, smaller than the previous case. As a consequence, about 37% of the total volume has a mean residence time greater than the average hydraulic retention time $\bar{t} = 3$ h. The intersection of the red curve with the vertical dashed line at $T_{res} = 30$ h shows a significant portion of estimated dead volume around 5% of the total reactor’s volume. Anyway, the location of such a dead volume can not be deduced from the curve in Fig. 4.

The estimates of dead volume obtained with the numerical model for both functioning conditions (i.e., “upstream mixing” and “no-mixing”) are in close accordance with the results obtained from the RTD method that are shown in Fig. 5.

The left-hand panel of Fig. 5 shows the results for the operating condition of upstream impeller turned on (“upstream mixing”). The asterisks denote the experimental samples of lithium concentration at the outflow of the oxidation/nitrification tank. The interpolating blue dashed curve has been obtained from the discrete model assuming neither bypass nor dead volume in the reactor series. The comparison between experimental data and the analytical curve shows good agreement. In particular, the discrete model allows simulating the rapid initial increase of the lithium concentration that rises to about 1.3 mg L^{-1} in the early 40 min of the test. Even the subsequent decay of lithium concentration in the outflow is suitably simulated, showing, immediately after the peak, a relatively small gap between experimental data and analytical results which reduces progressively.

The right-hand panel of Fig. 5 compares experimental data (red plus markers) and calculated (continuous blue line) time evolution of the outflow lithium concentration for the functioning condition corresponding to absence of mixing in both tanks. When considering no bypass and assuming 5% dead volume in the reactor, the discrete model can simulate the measured peak concentration of 1.32 mg L^{-1} , even if it is shifted forward of about 50 min with respect to the experimental peak; this is due to the fact that the lithium concentration sampled at the outflow of the oxidation/nitrification tank rise very fast in time while the slope of the ascending tract of the analytical curve is more mild. It can be seen that the lithium concentration decay of the samples immediately after the peak is more rapid than the analytical curve, thus producing major discrepancy in the time interval $2 \text{ h} < t < 4 \text{ h}$; conversely, the tail of the analytical curve is more close to the experimental points. The obtained interpolation of experimental samples is, however, satisfactory for practical applications to plant management, and therefore, the estimate of 5% dead volume resulting from the RTD analysis can be considered representative of the actual hydrodynamic behavior of the reactor in absence of mixing.

Both RTD and CFD analysis have shown that when the upstream impeller is turned on, about 96% of the total volume has a mean residence time lower than the average hydraulic retention time, and therefore, no significant dead volume can be detected. Conversely, when

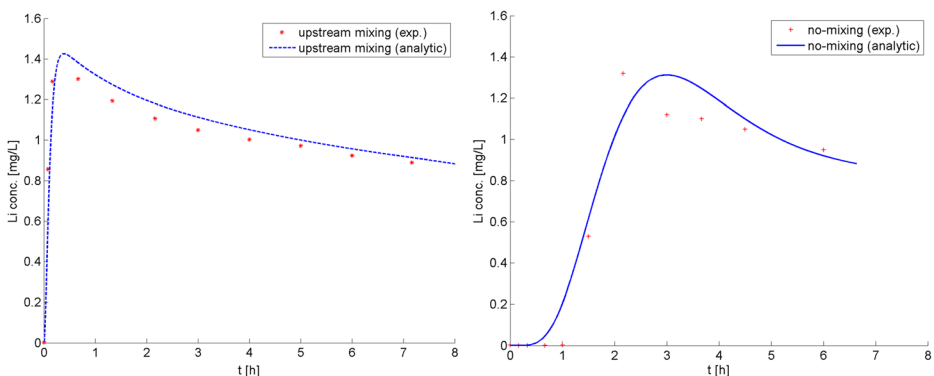


Fig. 5 Experimental and calculated time evolution of outflow lithium concentration for both operating conditions: “upstream mixing” on the left-hand panel, and “no-mixing” on the right-hand panel

both impellers are turned off (i.e., “no-mixing” condition) RTD and CFD analysis furnish similar estimate of the percentage of dead volume which is about 5%.

Information regarding the position of such a dead volume in the “no-mixing” case can be obtained from the streamlines of the fluid particles plotted in Fig. 6. The left-hand panel shows the velocity magnitude, while the right-hand panel indicates the distribution of the calculated residence time.

When considering the upstream denitrification compartment, it can be seen that the velocity magnitude is almost equal to $1.0\text{E-}4 \text{ m s}^{-1}$ across the whole length with the exception of the left-hand side of the tank which is far from the bottom opening connecting with the oxidation/nitrification tank: in this zone, the velocity modulus reduces by one order of magnitude, thus denoting possible stagnation. However, the characteristics of the flow pattern in the upstream compartment seem to exclude the formation of significant dead volume in the denitrification tank.

Concerning the downstream oxidation/nitrification compartment, one can notice two volumes characterized by a very small velocity magnitude. The greater volume is placed in the upper left-hand corner of the compartment where the velocity modulus reduces to about $1.0\text{E-}7 \text{ m s}^{-1}$. A smaller volume, where the particles velocity is of the same order of magnitude, is located at the lower right-hand corner of the compartment. As it can be seen from the right-hand panel of Fig. 6, the calculated residence time in these two zones is of the order of 10 h or greater, and denotes the presence of dead volumes. This is confirmed by the contour plot of the calculated residence time which is shown in Fig. 7. In this figure are shown the traces on the domain boundaries of those zones where the retention times exceed 30 h: it can be seen that the major portion of dead volume is placed in the upper left-hand side of the oxidation/nitrification tank. This result seems reasonable since this region lies far from the outflow section that attracts the fluid particles from the tank bottom toward the upper-right side. As a consequence, the velocity modulus of the fluid particles is very close to zero in the upper left-hand side of the oxidation/nitrification tank (Fig. 6) and stagnation occurs in this zone.

The results in Fig. 7 show that some smaller portions of dead volume are located at the lower right-hand corner of the downstream compartment and at the lower left-hand corner of the upstream compartment. This is in accordance with the global hydrodynamic path of the

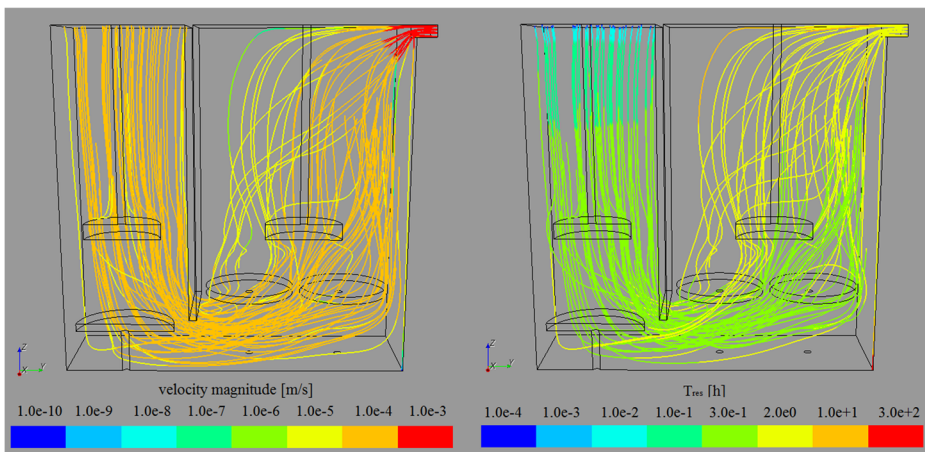


Fig. 6 Streamlines of fluid particles in the reactor (“no-mixing”). Color map shows velocity magnitude (left-hand panel) and residence time (right-hand panel)

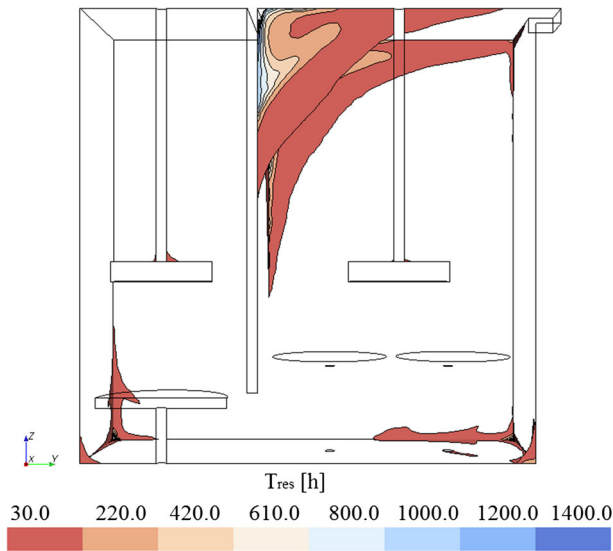


Fig. 7 Distribution of dead volume at the boundaries of the domain ($T_{res} > 30$ h, “no-mixing”)

fluid particles shown in Fig. 6. In fact, in the upstream tank, the descending fluid deviates toward the right-hand vertical opening close to the bottom, thus creating a stagnant zone at the lower left-hand corner; similarly, in the downstream tank the fluid exiting from the vertical opening close to the bottom is attracted toward the upper outflow section and does not reach the lower right-hand corner where a small dead volume is forming.

In accordance with the work by Le Moullec et al. (2010a), the obtained results have shown that CFD can be a useful and convenient tool for investigating the hydrodynamics of a wastewater treatment reactor when time-consuming kinetic models are not accounted. In particular, when performing hydrodynamic assessment of the reactor, CFD allows obtaining reliable information about the defects due to bypass and dead volume with low computational effort.

Even if in some kind of hydrodynamic investigations the choice of the turbulence model may affect the accuracy of the numerical results (Le Moullec et al. 2008), in the studied case the adoption of standard $k-\varepsilon$ model has allowed to obtain reliable hydrodynamic representation of the flow field for the analysis of the reactor performance, as confirmed by the comparison with the experimental results.

In order to obtain preliminary information on the behavior of the numerical model when biomass is suspended inside the reactor’s water, an additional simulation has been carried out considering a non-Newtonian fluid.

The adopted CFD code allows the choice among some available non-Newtonian generalized models: even if these models are available also for turbulent flows, it should be noted that turbulence models have been originally ideated for Newtonian fluids. Therefore, the physical consistency of the obtained results should be carefully checked and validated through comparison with experimental tests. These tests are still in progress and the validation of the hydrodynamic model for a non-Newtonian sludge will be the subject of a future study.

The suspended solid concentration affects the hydrodynamic behavior (and possibly the dead volume) of the reactor and influences the rheological behavior of the sludge that deviates from the Newtonian model. In order to point out these effects, a concentrated biomass has been

considered with total solids concentration of 150 gTSS L^{-1} from a thermophilic aerobic membrane reactor (TAMR) operating at $49 \pm 3 \text{ }^\circ\text{C}$ and pH of 7.6 ± 0.8 in a full scale plant (Collivignarelli et al. 2015a, b; Collivignarelli et al. 2017b). This solid concentration is significantly higher with respect to the biomass concentration usually adopted in conventional activated sludge (CAS) plants that is about one order of magnitude lower.

The Herschel-Bulkley model has been adopted to simulate the non-Newtonian fluid because it allowed describing the flow curve of several types of activated sludge with high solid concentration (Abbà et al. 2017). This model can be mathematically described by a power-law curve with an offset to account for possible yield stress τ_y . The rheological parameters adopted in the simulation have been obtained from experimental analysis of the adopted sludge and are the following: consistency coefficient $K = 3.39\text{E-}05 \text{ Pa s}^n$, flow behavior index $n = 2.725$ and yield stress $\tau_y = 0 \text{ Pa}$.

The numerical simulation has been carried out for isothermal stationary flow conditions. The remaining model features are the same adopted for the case of Newtonian fluid.

Figure 8 shows the results obtained considering no-mixing operating condition and compares the distribution curves of the mean residence time as percentage of reactor volume for Newtonian fluid (blue dashed line) and non-Newtonian fluid (continuous red line). It can be seen that for a mean residence time lower than 10 h, the distribution curves are very close to each other. On the contrary, the distribution curve of the non-Newtonian fluid is significantly higher for values of the mean residence time greater than 10 h, leading to an increase of about 40% in the estimate of dead volume with respect to the estimate obtained for the Newtonian fluid. For non-Newtonian fluid, the spatial distribution of the dead volume is analogous to the case of Newtonian fluid, but the spatial extension is increased.

These results need experimental validation in order to evaluate their degree of reliability. Anyway, they seem reasonable from a theoretical point of view because the

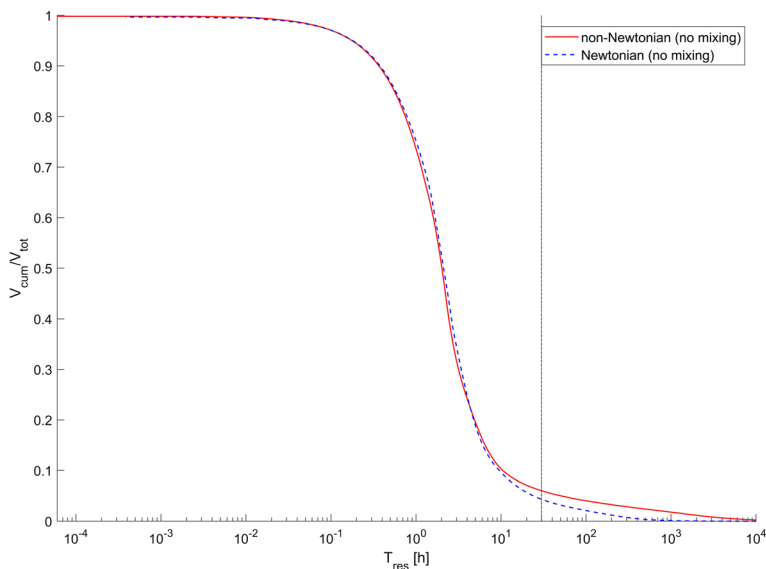


Fig. 8 Distribution curves of mean residence time as percentage of reactor volume for Newtonian and non-Newtonian fluids with “no-mixing” operating conditions

rheological model denotes a shear thickening (dilatant) behavior and the apparent viscosity increases with shear rate ($n > 1$).

4 Conclusions

In this work an integrated RTD – CFD analysis for assessing the hydrodynamic behavior of a biological reactor has been illustrated. Such reactor is part of a plant at pilot scale reproducing a common process scheme widely adopted in civil and industrial WWTPs. The reactor consists of two in-series compartments: the upstream compartment is devoted to denitrification, while the downstream compartment is used for oxidation/nitrification process.

At this stage of investigation, clear water has been considered for carrying out RTD experimental analysis of the pilot plant because this work aims at investigating the hydrodynamic behavior of the reactor that affects significantly the treatment efficiency. The aeration has not been considered, due to the absence of biochemical reactions. These assumptions allow reducing the complexity of the numerical modeling that simulates the reactor's hydrodynamics assuming Newtonian single-phase flow.

Two distinct operating conditions have been considered for evaluating the influence of mixing: i) absence of mixing in both compartments of the reactor and ii) activation of the upstream impeller (inside the denitrification compartment).

The stimulus-response experimental test has been carried out through a pulse injection of non-reactive tracer at the inflow of the reactor and measuring the concentration at the outflow. The RTD curve has been interpolated from experimental data using a discrete tank-in-series model that allows estimating possible hydrodynamic problems. The results have shown absence of bypass for both operating conditions; only when both impellers are turned off a significant percentage of dead volume (about 5%) has been detected.

The 3D hydrodynamic analysis with the finite volume model has confirmed the experimental results; when both impellers are turned off, the same percentage of dead volume (about 5%) as in the RTD analysis has been found.

The numerical model has revealed that the significant part of dead volume is confined in the upper-left corner of the oxidation/nitrification tank, in accordance with the global hydrodynamic path of the fluid particles obtained from the analysis.

An attempt to account for the presence of the sludge has been made by simulating non-Newtonian fluid. The numerical model has shown that the non-Newtonian model affects the amount of dead volume, while its spatial distribution remains unchanged. Anyway, the development of reliable non-Newtonian hydrodynamic model requires validation with experimental data, and therefore, this will be the subject of a future study to account for the actual behavior of the sludge.

The integrated use of RTD – CFD analysis proved to be effective in defining the types of hydrodynamic defects and their position inside the reactor. The obtained information can support the planning of proper corrective interventions that will increase the process efficiency and reliability. In particular, the numerical model can be used in a future research to investigate the effect of possible modifications of the tank geometry in order to reduce the extent of stagnant regions.

Acknowledgements An initial shorter version of the paper has been presented at the 10th World Congress of the European Water Resources Association (EWRA2017) “Panta Rhei”, Athens, Greece, 5-9 July, 2017 (<http://ewra2017.ewra.net/>).

The authors wish to thank “ASMia S.r.l.” (Mortara, Pavia) water company for its collaboration during the experimental work.

References

- Abbà A, Collivignarelli MC, Manenti S, Pedrazzani R, Todeschini S, Bertanza G (2017) Rheology and microbiology of sludge from a thermophilic aerobic membrane reactor. *J Chem Article ID 8764510*. <https://doi.org/10.1155/2017/8764510>
- APHA, AWWA, WEF (2012) Standard methods for the examination of water and wastewater, 22nd edn. American Public Health Association, Washington DC
- Baléo JN, Le Cloirec P (2000) Validating a prediction method of mean residence time spatial distributions. *AICHE J* 46:675–683. <https://doi.org/10.1002/aic.690460403>
- Bertanza G, Collivignarelli C (2006) The functional tests for the optimization of urban wastewater treatment plants (Le verifiche di funzionalità per l’ottimizzazione della depurazione delle acque di scarico urbane). *Collana Ambiente – volume 28*. CIPA edn, Milano. ISSN: 1121-8215 (in italian)
- Bertanza G, Papa M, Canato M, Collivignarelli MC, Pedrazzani R (2014) How can sludge dewatering devices be assessed? Development of a new DSS and its application to real case studies. *J Environ Manag* 137:86–92. <https://doi.org/10.1016/j.jenvman.2014.02.002>
- Brouckaert CJ, Buckley CA (1999) The use of computational fluid dynamics for improving the design and operation of water and wastewater treatment plants. *Water Sci Technol* 40:81–89. [https://doi.org/10.1016/S0273-1223\(99\)00488-6](https://doi.org/10.1016/S0273-1223(99)00488-6)
- Collivignarelli C, Bina S (1993) The hydrodynamic behaviour of an anaerobic digester for domestic sludge: comparative tests. *Eur Water Pollut Control* 3:9–12
- Collivignarelli C, Bertanza G, Bina S (1995) Hydrodynamic tests in the water treatment - theoretical basis, application procedures, examples (La verifica idrodinamica nel trattamento delle Acque - Basi teoriche, procedure di applicazione, esempi). *Collana Ambiente – volume 8*. CIPA edn, Milano. ISSN: 1121-8215 (in italian)
- Collivignarelli C, Pergetti M, Riganti V (2000) The management of wastewater treatment plants. Proposals of guidelines for the maintenance, control, verification, upgrading and co-treatment with aqueous special waste (La gestione degli impianti di depurazione delle acque di scarico. Proposte di linee guida per la manutenzione, il controllo, le verifiche, l’upgrading e i trattamenti congiunti di reflui speciali). *Il sole 24Ore* edn., Milano. ISBN: 88-324-4047-4 (in italian)
- Collivignarelli MC, Abbà A, Bertanza G (2015a) Why use a thermophilic aerobic membrane reactor for the treatment of industrial wastewater/liquid waste? *Environ Technol* 36:2115–2124. <https://doi.org/10.1080/09593330.2015.1021860>
- Collivignarelli MC, Bertanza G, Sordi M, Pedrazzani R (2015b) High-strength wastewater treatment in a pure oxygen thermophilic process: 11-year operation and monitoring of different plant configurations. *Water Sci Technol* 71:588–596. <https://doi.org/10.2166/wst.2015.008>
- Collivignarelli MC, Abbà A, Alloisio G, Gozio E, Benigna I (2017a) Disinfection in wastewater treatment plants: evaluation of effectiveness and acute toxicity effects. *Sustainability* 9:1704. <https://doi.org/10.3390/su9101704>
- Collivignarelli MC, Abbà A, Castagnola F, Bertanza G (2017b) Minimization of municipal sewage sludge by means of a thermophilic membrane bioreactor with intermittent aeration. *J Clean Prod* 143:369–376. <https://doi.org/10.1016/j.jclepro.2016.12.101>
- De Gussem K, Fenu A, Wambeq T, Weemaes M (2014) Energy saving on wastewater treatment plants through improved online control: case study wastewater treatment plant Antwerp-south. *Water Sci Technol* 69:1074–1079. <https://doi.org/10.2166/wst.2014.015>
- Do-Quang Z, Cockx A, Line A, Roustan M (1998) Computational fluid dynamics applied to water and wastewater treatment facility modeling. *Environ Eng Policy* 1:137–147. <https://doi.org/10.1007/s100220050015>
- Essemiani K, Vermande S, Marsal S, Phan L, Meinhold J (2004) Optimization of WWTP units using CFD – a tool grown for real scale application. In: Van Loosdrecht M, Clement J (eds.), 2nd IWA leading-edge conference on water and wastewater treatment technologies. IWA Publishing, London, pp. 183–192

- Gallati M, Bertanza G, Sibilla S, Collivignarelli MC, Gazzola E (2007) Integrated test to assess the hydrodynamic behavior of a biological reactor using RTD and numerical models (Verifica integrata del comportamento idrodinamico di un reattore biologico mediante metodo RTD e modelli numerici). *IA Ingegneria Ambientale* XXXVI:392–403 in italian
- Guimet V, Savoye P, Audic JM, Do-Quang Z (2004) Advanced CFD tool for wastewater: today complex modelling and tomorrow easy-to-use interface. In: van Loosdrecht M, Clement J (eds) 2nd IWA leading-edge conference on water and wastewater treatment technologies. IWA Publishing, London, pp 165–172
- Hirt CW, Nichols BD (1981) Volume of fluid (VOF) method for the dynamics of free boundaries. *J Comput Phys* 39:201–225. [https://doi.org/10.1016/0021-9991\(81\)90145-5](https://doi.org/10.1016/0021-9991(81)90145-5)
- Hreiz R, Latifi MA, Roche N (2015) Optimal design and operation of activated sludge processes: state-of-the-art. *Chem Eng J* 281:900–920. <https://doi.org/10.1016/j.cej.2015.06.125>
- Karama AB, Onyejekwe OO, Brouckaert CJ, Buckley CA (1999) The use of computational fluid dynamics (CFD) technique for evaluating the efficiency of an activated sludge reactor. *Water Sci Technol* 39:329–332. [https://doi.org/10.1016/S0273-1223\(99\)00294-2](https://doi.org/10.1016/S0273-1223(99)00294-2)
- Karpinska AM, Bridgeman J (2016) CFD-aided modelling of activated sludge systems. A critical review. *Water Res* 88:861–879. <https://doi.org/10.1016/j.watres.2015.11.008>
- Kjellstrand R, Mattsson A, Niklasson C, Taherzadeh MJ (2005) Short circuiting in a denitrifying activated sludge tank. *Water Sci Technol* 52:79–87
- Kochevsky AN (2004) Possibilities of simulation of fluid flows using the modern CFD software tools. Cornell University Library, <https://arxiv.org/abs/physics/0409104v1>
- Lauder BE, Spalding DB (1974) The numerical computation of turbulent flows. *Comput Methods Appl Mech Eng* 3:269–289. [https://doi.org/10.1016/0045-7825\(74\)90029-2](https://doi.org/10.1016/0045-7825(74)90029-2)
- Laurent J, Samstag RW, Ducoste J, Griborio A, Nopens I, Batstone DJ, Wicks J, Saunders S, Potier O (2014) A protocol for the use of computational fluid dynamics as a supportive tool for wastewater treatment plant modelling. *Water Sci Technol* 70:1575–1584. <https://doi.org/10.2166/wst.2014.425>
- Le Moulec Y, Potier O, Gentric C, Leclerc JP (2008) Flow field and residence time distribution simulation of a cross-flow gas–liquid wastewater treatment reactor using CFD. *Chem Eng Sci* 63:2436–2449. <https://doi.org/10.1016/j.ces.2008.01.029>
- Le Moulec Y, Gentric C, Potier O, Leclerc JP (2010a) Comparison of systemic, compartmental and CFD modeling approaches: application to the simulation of a biological reactor of wastewater treatment. *Chem Eng Sci* 65:343–350. <https://doi.org/10.1016/j.ces.2009.06.035>
- Le Moulec Y, Gentric C, Potier O, Leclerc JP (2010b) CFD simulation of the hydrodynamics and reactions in an activated sludge channel reactor of wastewater treatment. *Chem Eng Sci* 65:492–498. <https://doi.org/10.1016/j.ces.2009.03.021>
- Levenspiel O (1999) *Chemical Reaction Engineering*, Third edn. Wiley, New York
- Manenti S, Pierobon E, Gallati M, Sibilla S, D’Alpaos L, Macchi E, Todeschini S (2016) Vajont disaster: smoothed particle hydrodynamics modeling of the postevent 2D experiments. *J Hydraul Eng* 142(4): 05015007. doi:[https://doi.org/10.1061/\(ASCE\)HY.1943-7900.0001111](https://doi.org/10.1061/(ASCE)HY.1943-7900.0001111)
- Manenti S, Todeschini S, Collivignarelli MC, Abbà A (2017) CFD-aided modelling for hydrodynamic analysis of biological reactor. Proc. 10th World Congress of EWRA, 5–9 July 2017 Athens (Greece). *Eur Water* 58: 47–51
- Meister M, Winkler D, Rezavand M, Rauch W (2017) Integrating hydrodynamics and biokinetics in wastewater treatment modelling by using smoothed particle hydrodynamics. *Comput Chem Eng* 99:1–12. <https://doi.org/10.1016/j.compchemeng.2016.12.020>
- Morchain J, Maranges C, Fonade C (2000) CFD modelling of a two-phase aerator under influence of a crossflow. *Water Res* 34:3460–3472. [https://doi.org/10.1016/S0043-1354\(00\)00080-4](https://doi.org/10.1016/S0043-1354(00)00080-4)
- Morchain J, Gabelle JC, Cockx A (2014) A coupled population balance model and CFD approach for the simulation of mixing issues in lab-scale and industrial bioreactors. *AICHE J* 60:27–40. <https://doi.org/10.1002/aic.14238>
- Nauman EB (2007) Residence time distributions. In: *Chemical Reactor Design, Optimization, and Scaleup*, Second edn. Wiley, Hoboken, pp 535–574
- Newell B, Bailey J, Islam A, Hopkins L, Lant P (1998) Characterising bioreactor mixing with residence time distribution (RTD) tests. *Water Sci Technol* 37:43–47. [https://doi.org/10.1016/S0273-1223\(98\)00000-6](https://doi.org/10.1016/S0273-1223(98)00000-6)
- Papa M, Bertanza G, Abbà A (2016) Reuse of wastewater: a feasible option, or not? A decision support system can solve the doubt. *Desalin Water Treat* 57:8670–8682. <https://doi.org/10.1080/19443994.2015.1029532>
- Patankar SV, Spalding DB (1972) A calculation procedure for heat, mass and momentum transfer in three-dimensional parabolic flows. *Int J Heat Mass Transf* 15:1787–1806. [https://doi.org/10.1016/0017-9310\(72\)90054-3](https://doi.org/10.1016/0017-9310(72)90054-3)
- Patel VC, Rodi W, Sheuerer G (1985) Turbulence models for near wall and low Reynolds number flows: a review. *AIAA J* 23:1308–1319. <https://doi.org/10.2514/3.9086>

- Pereira JP, Karpinska AM, Gomes PJ, Martins AA, Dias MM, Lopes JCB, Santos RJ (2012) Activated sludge models coupled to CFD simulations. In: Single and Two-Phase Flows on Chemical and Biomedical Engineering. Eds: Dias MM, Lima R, Martins AA, Mata TM. Bentham Science Publishers Ltd, pp 153–173. <https://doi.org/10.2174/97816080529501120101>
- Raboni M, Gavasci R, Viotti P (2015) Influence of denitrification reactor retention time distribution (RTD) on dissolved oxygen control and nitrogen removal efficiency. *Water Sci Technol* 72:45–51. <https://doi.org/10.2166/wst.2015.188>
- Rodi W (1980) Turbulence Models and their Application in Hydraulics - a State of the Art Review, Third edn. A.A. Balkema, Rotterdam
- Sandberg M (1981) What is ventilation efficiency? *Build Environ* 16:123–135. [https://doi.org/10.1016/0360-1323\(81\)90028-7](https://doi.org/10.1016/0360-1323(81)90028-7)
- Sorlini S, Collivignarelli MC, Castagnola F, Crotti BM, Raboni M (2015a) Methodological approach for the optimization of drinking water treatment plants' operation: a case study. *Water Sci Technol* 71:597–604. <https://doi.org/10.2166/wst.2014.503>
- Sorlini S, Collivignarelli MC, Canato M (2015b) Effectiveness in chlorite removal by two activated carbons under different working conditions: a laboratory study. *J Water Supply: Res Technol – AQUA* 64:450–461. <https://doi.org/10.2166/aqua.2015.132>
- Sorlini S, Biasibetti M, Collivignarelli MC, Crotti BM (2015c) Reducing the chlorine dioxide demand in final disinfection of drinking water treatment plants using activated carbon. *Environ Technol* 36:1499–1509. <https://doi.org/10.1080/09593330.2014.994043>
- Todeschini S (2012) Trends in long daily rainfall series of Lombardia (Northern Italy) affecting urban stormwater control. *Int J Climatol* 32(6):900–919. <https://doi.org/10.1002/joc.2313>
- Todeschini S (2016) Hydrologic and environmental impacts of imperviousness in an industrial catchment of northern Italy. *J Hydrol Eng* 21(7):05016013. [https://doi.org/10.1061/\(ASCE\)HE.1943-5584.0001348](https://doi.org/10.1061/(ASCE)HE.1943-5584.0001348)
- Todeschini S, Ciaponi C, Papiri S (2010) Laboratory experiments and numerical modelling of the scouring effects of flushing waves on sediment beds. *Eng Appl Comput Fluid Mech* 4(3):365–373
- Todeschini S, Papiri S, Sconfiotti R (2011) Impact assessment of urban wet-weather sewer discharges on the Vernavola river (Northern Italy). *Civ Eng Environ Syst* 28(3):209–229. <https://doi.org/10.1080/10286608.2011.584341>
- Todeschini S, Papiri S, Ciaponi C (2012) Performance of stormwater detention tanks for urban drainage systems in northern Italy. *J Environ Manag* 101:33–45. <https://doi.org/10.1016/j.jenvman.2012.02.003>
- Warhaft Z (2000) Passive scalars in turbulent flows. *Annu Rev Fluid Mech* 32:203–240. <https://doi.org/10.1146/annurev.fluid.32.1.203>